Environmental Science: Atmospheres

ROYAL SOCIETY OF CHEMISTRY

PAPER

View Article Online
View Journal | View Issue

Cite this: *Environ. Sci.: Atmos.*, 2024, **4**, 942

Carbon and nitrogen-based gas fluxes in subarctic ecosystems under climate warming and increased cloudiness†

Flobert A. Ndah, *[a] Marja Maljanen, [a] Riikka Rinnan, [bc] Hem Raj Bhattarai, [ad] Cleo L. Davie-Martin, [b] Santtu Mikkonen, [ae] Anders Michelsen [b] and Minna Kivimäenpää [af]

Climate warming is projected to be particularly pronounced in the northern high latitudes coupled with reduced light availability due to increased cloudiness. The changing climate may alter the fluxes of greenhouse gases (GHGs) and atmospherically reactive trace gases, which can drive important climate feedbacks. We investigated the individual and combined effects of warming and increased cloudiness on methane (CH_4), carbon dioxide (CO_2), nitrous oxide (N_2O), nitric oxide (NO), nitrous acid (HONO) and biogenic volatile organic compound (BVOC) fluxes in mesocosms from two tundra and one palsa mire ecosystems kept under strict environmental control in climate chambers. We also examined whether and how prevailing soil physiochemical properties and plant species composition affected the fluxes. In control conditions, all sites were net sinks of CH_4 and CO_2 during both growing seasons except for the palsa site which was a net source of CO_2 in the second growing season. Warming enhanced CH_4 uptake, mostly observed in the palsa site, and turned the palsa site from a sink to a source of CO_2 in the first growing season and increased the CO_2 source strength in the second growing season. Warming increased BVOC emissions while increased cloudiness mostly decreased the emissions. The combined treatment of warming and increased cloudiness decreased CH_4 uptake, mostly observed in the palsa site, and BVOC emissions. Fluxes of CO_2 were linked to availability of soil carbon and organic matter, litter input, soil pH and bulk density, and cover of mosses. Low emissions of N_2O, NO, and HONO could mainly be explained by limited availability of mineral nitrogen. Warming-enhanced CH_4 uptake and BVOC emissions will provide a negative feedback to climate while enhanced CO_2 release from palsa mires will exacerbate global warming. Under combined warming and increased cloudiness, subarctic ecosystems may shift from sinks to sources of CH_4, providing a positive feedback to climate. Prevailing soil physiochemical properties and vegetation composition will play a significant role in controlling the fluxes, hence contributing to the overall climate change effects and feedback.

Received 30th January 2024
Accepted 9th July 2024

DOI: 10.1039/d4ea00017j

rsc.li/esatmospheres

Environmental significance

The high latitudes of the Northern Hemisphere are warming at a rate faster than the global average coupled with reduced light availability due to increased cloudiness. We have an inadequate understanding of how the rapidly changing climate will affect the ecosystem–atmosphere exchange of trace gases in the northern high latitudes which can have important feedback effects on the climate. Here, using a climate chamber setup, we quantified fluxes of greenhouse and atmospherically reactive trace gases in mesocosms from two tundra and one palsa mire ecosystems exposed to simulated conditions of future warming and increased cloudiness in the Subarctic. The palsa mire was the most responsive to the climate treatments as warming enhanced methane uptake and emissions of biogenic volatile organic compounds suggesting these ecosystems will provide a negative feedback to climate. Palsa mires will also be stronger carbon dioxide sources under warming and in the long term may shift from sinks to sources of methane under combined warming and increased cloudiness, providing a positive feedback to climate.

[a]*Department of Environmental and Biological Sciences, University of Eastern Finland, P. O. Box 1627, 70211 Kuopio, Finland. E-mail: flobert.ndah@uef.fi*

[b]*Department of Biology, Terrestrial Ecology Section, University of Copenhagen, 2100 Copenhagen Ø, Denmark*

[c]*Department of Biology, Center for Volatile Interactions (VOLT), University of Copenhagen, 2100 Copenhagen Ø, Denmark*

[d]*Natural Resources Institute Finland, Halolantie 31 A, FI-71750, Maaninka, Finland*

[e]*Department of Technical Physics, University of Eastern Finland, P. O. Box 1627, 70211 Kuopio, Finland*

[f]*Natural Resources Institute Finland, Juntintie 154, 77600 Suonenjoki, Finland*

† Electronic supplementary information (ESI) available. See DOI: https://doi.org/10.1039/d4ea00017j

1. Introduction

Carbon and nitrogen cycling involve a range of processes exchanging trace gases between ecosystems and the atmosphere, which govern the net carbon balance.[1–3] We have an inadequate understanding of how the ecosystem–atmosphere exchange of different trace gases in the high latitude northern ecosystems is affected by the rapidly changing climate.

Methane (CH_4) and carbon dioxide (CO_2) are greenhouse gases (GHGs), the fluxes of which are controlled by both biotic and abiotic processes.[4,5] In anoxic conditions, CH_4 is produced through methanogenesis by anaerobic microorganisms of the Archaea domain.[6] The produced CH_4 is then transported to the atmosphere by molecular diffusion, plant-mediated transport, or ebullition, and during this transport part of the CH_4 is consumed through oxidation by methanotrophic bacteria in well-aerated soils.[5–7] The net exchange of CO_2 between terrestrial ecosystems and the atmosphere is determined by the balance between photosynthesis and respiration. 'Carbon-fixing' autotrophic organisms, mainly plants and photosynthetic soil microbes, take up CO_2.[8] Fixed carbon is then returned to the atmosphere (emission) *via* plant and soil respiration.[8] The fluxes of CH_4 and CO_2 are affected by plant species composition and soil properties such as soil temperature, soil moisture and permeability, nutrient availability, and soil pH,[1,4,5,7,9–12] while solar radiation and temperature are the main drivers of CO_2 uptake and emission.[13]

Nitrous oxide (N_2O) is a potent GHG, which has 273 times stronger warming potential than CO_2 in 100 year's reference period.[14] Nitric oxide (NO) is readily oxidized by ozone (O_3) in the atmosphere, and it plays a vital role in maintaining the atmospheric O_3 level.[15] Nitrous acid (HONO) is an important source of hydroxyl (OH) radicals in the atmosphere, contributing *ca.* 55% of total daytime OH production,[16] which can reduce the atmospheric lifetime of CH_4 through oxidation.[17] The fluxes of the nitrogenous gases N_2O, NO, and HONO at soil–atmosphere interphase are related to biotic (*e.g.* nitrification or denitrification) and abiotic (chemodenitrification) processes.[18–20] Also, soil moisture and pH, and the availability of mineral nitrogen such as nitrate (NO_3^-), nitrite (NO_2^-) and ammonium (NH_4^+) essential for nitrification, denitrification, and chemodenitrification processes are important factors governing the fluxes of N_2O, NO, and HONO.[18–22]

Plants emit substantial amounts of their photosynthetically assimilated carbon to the atmosphere as biogenic volatile organic compounds (BVOCs).[23] BVOCs are a diverse group of non-methane hydrocarbons, and they are also released from soils.[24] BVOCs are involved in defense against abiotic and biotic stresses and in plant–insect–microbe interactions.[24,25] BVOCs are reactive compounds and, together with NO and HONO, play a significant role in atmospheric chemistry. BVOCs contribute to the formation of tropospheric O_3 by interacting with NO_x under sunlight.[15] In Arctic and subarctic regions where NO_x levels are relatively low, BVOCs mainly react with OH radicals and photo-oxidation of BVOCs by OH radicals can increase the atmospheric lifetime of CH_4.[26] Photo-oxidation of BVOCs further leads to the formation of secondary organic aerosols, which are precursors of cloud formation and may exert net cooling (*i.e.* negative radiative) effect on the climate.[27,28]

Climate change is projected to be particularly pronounced in high-latitude regions.[14] Mean annual temperature in the northern high latitudes has already increased by 2–3 °C since the 1950s,[29] and the increase by 2050 is projected to be about 4 °C.[30] Besides warming, the northern high latitudes will also experience changes in precipitation, evaporation patterns, and cloud cover.[14,31] The warmer conditions together with increased cloudiness will likely directly influence the ecosystem–atmosphere fluxes of greenhouse and atmospherically reactive gases in the subarctic region.

Warming could lead to enhanced decomposition and mineralization, which may increase the release of carbon-based compounds such as CH_4, CO_2, or BVOCs to the atmosphere, triggering important feedback loops.[14,32–34] Warming-induced enhanced plant growth and changes in plant community composition and extent in the high latitudes[35,36] will increase photosynthetic uptake of CO_2.[32,37] Increased inputs of deciduous leaf litter can affect nutrient content, substrate availability, and microbial community structure and activity,[35,38–40] which in turn influence gas fluxes. Warming may also enhance soil nitrification and denitrification processes,[41] which are important pathways of soil N_2O, NO, and HONO production.[18–20] Since BVOC emissions from northern vegetation and soils are highly temperature sensitive,[42–44] drastically increased emissions from vegetation and soil are expected under the projected climate warming of 4 °C by 2050. Increased cloudiness due to increased moisture content of a warmer atmosphere will reduce the solar radiation reaching the Earth's surface.[45,46] As emissions of many BVOCs are light-dependent,[47,48] reduced incoming radiation has the potential to decrease the emissions.

Understanding how warming and increased cloudiness alone and in concert affect the fluxes of GHGs and reactive trace gases in subarctic ecosystems is essential for the projection of future climate change effects and feedback. Here we investigated how the fluxes of CH_4, CO_2, N_2O, NO, HONO, and BVOCs in mesocosms of three subarctic ecosystems are altered by climate change, specifically focusing on the effects of increased temperature, increased cloudiness, and the interaction between these two. We also examined whether and how vegetation (plant species composition) and soil properties affect the fluxes.

2. Materials and methods

2.1 Mesocosm sampling, experimental setup, and climate simulation

Mesocosms, *i.e.* blocks of soil and the intact vegetation on top, were collected from three subarctic ecosystem sites in August 2019. The mesocosms were collected into PVC cylinders (inner ø 18 cm, h 15 cm). A total of 20 mesocosms were collected per site giving a total of 60 mesocosms from all sites. The collection sites were a heath tundra in Vassijaure (68°25′45″N, 18°15′37″E, 550 m a.s.l.), northern Sweden, where collection was done from two locations that appeared different in soil fertility based on vegetation composition, and a palsa mire in Kilpisjärvi (68°

53′4.5″N, 21°3′10.7″E), northern Finland. The tundra sites are hereafter referred to as the T1 and T2 sites and the palsa mire as the P site. The tundra sites (T1 and T2) were dominated by deciduous shrubs, graminoids, and forbs, with mosses and lichens covering the ground layer; the more fertile T1 had higher cover of graminoids and forbs but lower cover of lichens than T2. The P site was dominated by evergreen shrubs with the ground layer covered by litter and patches of bare peat. The tundra sites were characterized by podsol soil formation while the palsa site was a peatland, with several meters of peat and with discontinuous permafrost underneath. Mesocosm collection, vegetation composition, and soil physiochemical properties at the sites have been described in detail by Ndah *et al.*[49] After collection, mesocosms were weighed and transported to the laboratory and regularly sprayed with distilled water to avoid desiccation. Prior to the start of the first and second growing seasons in 2020 and 2021, respectively, mesocosms were maintained at +4 °C in a well-ventilated dark room to achieve plant dormancy occurring in (sub)arctic winter under snow.

Mesocosms were grown in four computer-controlled climate chambers, allowing the simulation of future summer temperature and increased cloud cover conditions in the subarctic. The experimental design consisted of four climate treatments: control (C), warming (W), increased cloudiness (−PAR) and warming + increased cloudiness (W−PAR). Five replicate mesocosms from each ecosystem site were randomly assigned to each climate treatment giving a total of 15 mesocosms per climate treatment. The climate chambers were equipped with 2 × Valoya G2 + 4 × Valoya NS1 LED luminaires (Valoya B100, Finland) at a height of 30 cm from the top of plant canopy. A mesh fabric (SEFAR NITEX® 03-50/37, Switzerland) was placed between the lamps and plant canopy top (about 5 cm below lamps and 25 cm above plant canopy top) to create diffuse light environment in the chambers since the northern high latitudes experience predominantly diffused rather than direct light due to the presence of frequent clouds coupled with atmospheric particles or pollutants. Climate data were collected from the Katterjåkk weather station (68°24′45″N, 18°08′13″E) which is closest to Vassijaure with similar climatic conditions. We used the 2010–2019 weekly average climate data of June, July, and August in Katterjåkk to simulate the summer climate in the control (C) chamber/treatment. We simulated the predicted warming scenario in the warming (W) chambers/treatments by increasing the air temperatures by 4 °C compared to the control. Irradiance conditions in the climate chambers were based on simulations of photosynthetically active radiation (PAR) and how it changes on a weekly basis according to the time of the day, *i.e.* solar elevation angle and cloud thickness during the months of June, July, and August in Katterjåkk. Control climate treatment was based on simulations with cloud optical depth of 10 and represented thin-cloud layer conditions. In the increased cloudiness treatments, PAR was decreased by 50% compared to the control and represented thick-cloud layer conditions (cloud optical depth of 30). The experimental setup and climate simulation have been described in detail by Ndah *et al.*[49] Mesocosms were exposed to the summer climate treatments in the chambers during two consecutive years (2020 and 2021) and for a three-month period (June–August) each year, averaging the length of the main growing season in the subarctic. Mesocosms were rotated within chambers on a weekly interval and mesocosms and treatments rotation between chambers was done on bi-weekly intervals to minimize chamber effects. Mesocosms were watered with distilled water to maintain their initial moisture level and weight.

2.2 Gas flux measurements and analyses

We performed mesocosm-scale measurements of gas fluxes during the two experimental growing seasons. Fluxes of CH_4, N_2O, and BVOCs were measured in six campaigns, and CO_2 and NO in five campaigns during the first growing season. Due to technical (device) constraints, HONO was measured in just two campaigns during the first growing season. Measurements were repeated at the same frequency during the second growing season for all gas fluxes, except for HONO which was not measured. Fluxes of CH_4, N_2O, HONO, and NO were measured at room temperature (+21 °C) by taking the mesocosms out from the climate chamber for the duration of measurements. Fluxes of CH_4 and N_2O were measured simultaneously with a static chamber (V = 4.8 L) system (ESI_1 Fig. S1†) and samples were analyzed for CH_4 and N_2O concentrations with a gas chromatograph (Agilent 7890B, Agilent Technologies, USA) equipped with a Gilson GX-271 autosampler (Gilson Inc, USA) (see ESI_1† for details). The fluxes of HONO and NO were measured simultaneously using a dynamic chamber (V = 3.2 L) system (ESI_1 Fig S2†) connected to a commercial long path absorption photometer (LOPAP) HONO analyzer (QUMA Elektronik & Analytik GmbH, Germany) for HONO and a Thermo 42i NO_x analyzer (Thermo Fisher Scientific, USA) for NO (see ESI_1† for details).

Sampling of CO_2 and BVOCs were conducted under the simulated growing conditions in the climate chambers. During sampling, the climate chamber door was closed, which ensured that light, temperature, and humidity stayed stable. Measurements of CO_2 exchange were conducted, using transparent enclosure chamber, with an EGM-4 infrared Environmental Gas Monitor (PP Systems, Hitchin, UK) connected to an Environmental Monitor Sensor Probe Type 3 (PP Systems, Hitchin, UK). Two measurements were conducted per mesocosm, one in light conditions (3 min) and one with the chamber covered with a dark cloth (3 min). A linear regression of the change in the CO_2 concentration in light was used as an estimate of net ecosystem exchange (NEE) and that in the dark of the dark ecosystem respiration (ER). The gross ecosystem production (GEP) was derived by subtracting ER from NEE. Measurements of BVOCs were conducted using a dynamic enclosure technique (ESI_1 Fig. S3†) and samples were analyzed using gas chromatography-mass spectrometry (Hewlett-Packard GC type 6890, Germany; MSD 5973, UK) (see ESI_1† for details). We categorized BVOCs into the following groups: isoprene, monoterpenes (MTs), oxygenated monoterpenes (oMTs), sesquiterpenes (SQTs), oxygenated sesquiterpenes (oSQTs), hydrocarbons (HCs), oxygenated VOCs (OVOCs), and other VOCs (ESI_1 Table S1†).

The fluxes of CH_4 and CO_2 are reported with negative values corresponding to uptake by the ecosystem, and positive values to emission from the ecosystem to the atmosphere.

2.3 Vegetation surveys and soil physiochemical properties

Mesocosm vegetation cover (%) was determined once at the end of the first growing season and four times during the second growing season. All plants were identified to species, with the exception of some lichens and mosses which were identified to genus, and then assigned to functional groups: evergreen shrubs, deciduous shrubs, graminoids, forbs, mosses, and lichens. The cover of litter + bare soil at the end of the first growing season, and litter, standing dead vegetation (*i.e.* dead vegetation with root connections), and bare soil during the second growing season were also assessed. Mesocosm soil physiochemical properties, such as the soil organic layer depth, organic matter content, bulk density, NO_3^-, NO_2^-, and NH_4^+ concentrations, pH, electrical conductivity, carbon and nitrogen content, total organic carbon content, gravimetric water content, and water holding capacity, were also analyzed at the end of the second growing season. Methods of vegetation surveys and analyses of soil physiochemical properties have been described in detail by Ndah *et al.*[49]

2.4 Statistical analyses

Mixed-models analysis of variance (ANOVA) (IBM SPSS Statistics 27.0.0, SPSS Inc. IBM Company ©, Armonk, NY, USA) was used to test for the effects of warming, increased cloudiness, site, time, and their interactions on the emissions of CH_4, CO_2, N_2O, and BVOC groups (isoprene, total MTs, total oMTs, total SQTs, total oSQTs, total HCs, total OVOCs, and total other VOCs). Warming, increased cloudiness, site, and time were included as fixed factors, whereas random factors included mesocosms as subjects. In addition, repeated measures type of setting was accounted with time. The final model was obtained by excluding nonsignificant (cutoff level 0.2) interactions, one by one, starting from the highest-level interactions and highest probability values.[50] The selection of covariance structure was based on the smallest Akaike's information criteria (AIC) and was set to either Diagonal (DIAG), Heterogenous compound symmetry (CSH) or Heterogenous autoregressive [ARH (1)]. The model residuals were checked by generating normality plots (histograms). In case the residuals were not normally distributed, the data were logarithmic or square-root-transformed. All interactions with P value < 0.1 were further tested for simple main effects (SME), *i.e.* post hoc test for interactions with Bonferroni corrections and SME P values < 0.05 were considered statistically significant.

Partial least squares regression (PLSR) was used to assess the covariance between the gas fluxes (dependent variables, Y) and the vegetation cover and soil physiochemical properties (independent variables, X) using SIMCA 17.0.2 (Umetrics, Umeå, Sweden). The PLSR were performed separately for each growing season using gas flux data, averaged across measurement campaigns, for the growing season. Vegetation data used for the first growing season analysis involved percentage cover of plant functional groups measured at the end of the season. For the second growing season, the average percentage cover of plant functional groups measured at the four time points during the season was used. One-component PLSR models were fitted separately for each gas following centering and unit variance scaling of the variables. Variables with VIP (Variable Influence on Projection) < 0.5 were excluded from the model. The significance of the models was tested using analysis of variance of the cross-validated residuals (CV-ANOVA).[51]

3. Results

3.1 Vegetation and soil physiochemical properties

Detailed results of vegetation and soil physiochemical properties have been presented by Ndah *et al.*[49] Briefly, all three study sites were acidic (pH 3.6–4.0). Mesocosms from the P site had higher organic layer depth on average (11 cm) than the T1 (7 cm) and T2 (4 cm) sites. Organic layer depth for T1 and T2 sites are representative of the field site conditions unlike the P site where the organic layer was several meters thick at field site. Soils from the P, T1, and T2 sites were made up of 97%, 87%, and 86% organic matter content, respectively. The soil gravimetric water content was 24%, 15%, and 13% for the P, T1, and T2 sites, respectively. The warming treatment increased biomass of one of the dominant evergreen shrubs *Empetrum hermaphroditum* while the cover of graminoids and forbs in the T1 site also increased in response to the combined warming and increased cloudiness treatments in the second growing season.

3.2 Methane fluxes

In the first growing season, CH_4 fluxes in control treatments across all measurement campaigns were in the range −36 to 52 μg CH_4–C m^{-2} h^{-1} for the T1 site, −97 to 109 μg CH_4–C m^{-2} h^{-1} for the T2 site, and −67 to 44 μg CH_4–C m^{-2} h^{-1} for the P site. Of all the measurements, 63% (T1 site), 67% (T2 site), and 70% (P site) exhibited negative CH_4 fluxes *i.e.* CH_4 uptake by the ecosystem. Across all treatments and sites, CH_4 fluxes varied significantly according to measurement campaign (P < 0.001; see ESI_1 text and Fig. S4†). Warming increased CH_4 uptake while the combined treatment decreased uptake, and these effects were particularly pronounced in the P site (W × −PAR × S × T interaction; see ESI_1 text, Table S3, and Fig. S5†).

The second growing season control treatment CH_4 fluxes were in the range −52 to 12 μg CH_4–C m^{-2} h^{-1} for the T1 site, −58 to 43 μg CH_4–C m^{-2} h^{-1} for the T2 site, and −133 to 72 μg CH_4–C m^{-2} h^{-1} for the P site. Of all the measurements, 58% (T1 site), 62% (T2 site), and 66% (P site) exhibited CH_4 uptake. Across all treatments and measurement campaigns, CH_4 flux differed significantly between the T1 and P sites (see ESI_1 text, Table S4, and Fig S6†). This was mainly due to the effects of warming alone which turned the T1 site from a sink to a source of CH_4 but increased CH_4 uptake rates and sink strength of the P site (W × −PAR × S interaction, Fig. 1, and ESI_1 Table S4†). However, in the combined treatment, both T1 and P sites were sinks of CH_4 (W × −PAR × S interaction, Fig. 1, ESI_1 Table S4†) and all three sites exhibited near zero fluxes (Fig. 1).

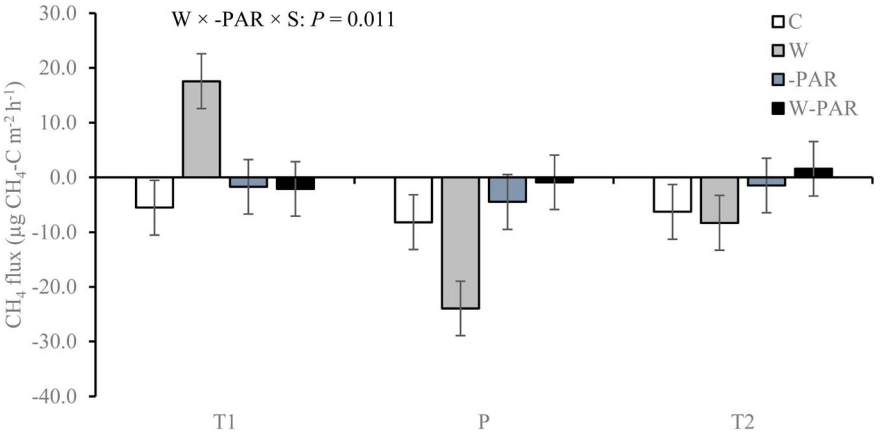

Fig. 1 CH_4 fluxes in mesocosms from T1, T2, and P sites under control (C), warming (W), increased cloudiness (−PAR), and warming + increased cloudiness (W−PAR) treatments across six measurement campaigns during the second growing season. Bars represent season mean values (±SE) measured from five replicate mesocosms per treatment and site. T = tundra, where T1 and T2 indicate the two locations within the tundra, and P = palsa mire. S = site and W × −PAR × S = warming × increased cloudiness × site interaction. Statistically significant *P*-values < 0.05 from LMM ANOVA are shown. See ESI_1 Table S4† for detailed statistics.

3.3 Carbon dioxide fluxes

During the first growing season, control treatment ER rates across all measurement campaigns were in the range 22 to 280 mg CO_2–C m^{-2} h^{-1} for the T1 site, 61 to 240 mg CO_2–C m^{-2} h^{-1} for the T2 site, and 46 to 4575 mg CO_2–C m^{-2} h^{-1} for the P site. Across all measurement campaigns, GEP fluxes in control treatments were in the range −7 to −323 mg CO_2–C m^{-2} h^{-1} for the T1 site, −100 to −320 mg CO_2–C m^{-2} h^{-1} for the T2 site, and −12 to −7626 mg CO_2–C m^{-2} h^{-1} for the P site. Across all measurement campaigns in control treatments, NEE averaged −67 ± 12 mg CO_2–C m^{-2} h^{-1} for the T1 site, −54 ± 10 mg CO_2–C m^{-2} h^{-1} for the T2 site, and −412 ± 205 mg CO_2–C m^{-2} h^{-1} for the P site. Of all NEE measurements, 98% exhibited negative CO_2 fluxes indicating mainly net CO_2 uptake by the ecosystem.

During the second growing season, control treatment ER rates were in the range 37 to 394 mg CO_2–C m^{-2} h^{-1} for the T1 site, 99 to 637 mg CO_2–C m^{-2} h^{-1} for the T2 site, and 139 to 9775 mg CO_2–C m^{-2} h^{-1} for the P site. Across all measurement campaigns, GEP fluxes in control treatments were in the range −73 to −836 mg CO_2–C m^{-2} h^{-1} for the T1 site, −12 to −1094 mg CO_2–C m^{-2} h^{-1} for the T2 site, and −46 to −8271 mg CO_2–C m^{-2} h^{-1} for the P site. Across all measurement campaigns in control treatments, NEE averaged −198 ± 39 mg CO_2–C m^{-2} h^{-1} for the T1 site, −154 ± 35 mg CO_2–C m^{-2} h^{-1} for the T2 site, and 81 ± 110 mg CO_2–C m^{-2} h^{-1} for the P site. Of all NEE measurements, 79% exhibited negative CO_2 fluxes, *i.e.* net CO_2 uptake by the ecosystem.

In both growing seasons, ER and GEP was higher in the P site than in the T1 and T2 sites (see ESI_1 text, Tables S3, S4, and Fig. S7†). In the first growing season, warming turned the P site from a net sink to a source of CO_2 (W × S interaction, Fig. 2a, and ESI_1 Table S3†). The P site also exhibited positive NEE fluxes (net source of CO_2) during the second growing season and warming significantly increased NEE (W × S interaction, Fig. 2b, ESI_1 Table S4†). Hence, the T1 and T2 sites were net sinks of CO_2 (negative NEE values) while the P site was a net source of CO_2 (positive NEE values).

3.4 Fluxes of nitrous oxide, nitric oxide, and nitrous acid

Across all measurement campaigns of the first growing season, N_2O emissions in control treatments were in the range 0.1 to 6.5 μg N m^{-2} h^{-1} for the T1 site, 0.4 to 6.2 μg N m^{-2} h^{-1} for the T2 site, and 1.2 to 5.8 μg N m^{-2} h^{-1} for the P site. Across all measurement campaigns of the second growing season, N_2O emissions in control treatments varied from 0.2 to 3.4 μg N m^{-2} h^{-1} for the T1 site, 0.2 to 4.7 μg N m^{-2} h^{-1} for the T2 site, and 0.2 to 4.4 μg N m^{-2} h^{-1} for the P site. There were no significant main or interaction effects of warming, increased cloudiness, site, and time on N_2O emissions during any of the growing seasons (data not shown). Emissions of NO and HONO were below detection limits (NO flux < 0.0004 μg N m^{-2} h^{-1} and HONO flux < 0.03 μg N m^{-2} h^{-1}).

3.5 Biogenic volatile organic compound fluxes

In both growing seasons, BVOC emissions comprised of isoprene, MTs, oMTs, SQTs, oSQTs, HCs, OVOCs, and other VOCs except that there were no isoprene emissions in mid-June of the first growing season. Emission rates of the individual compounds identified from mesocosms from each of the studied sites during both growing seasons are shown in the ESI_2.† Of all the BVOC groups in the first growing season, HCs, OVOCs, and SQTs comprised the largest fractions, contributing 34%, 30%, and 22%, respectively, of the total BVOC emissions averaged across all treatments, sites, and measurement campaigns (ESI_1 Fig. S8†). In the second growing season, the total BVOC emissions averaged across all treatments, sites, and measurement campaigns were largely dominated by SQTs (42%), HCs (34%) and OVOCs (17%) (ESI_1 Fig. S8†). In the first growing season, total BVOC emissions in control treatments averaged 57.7 ± 6.6 μg m^{-2} h^{-1} across all sites and

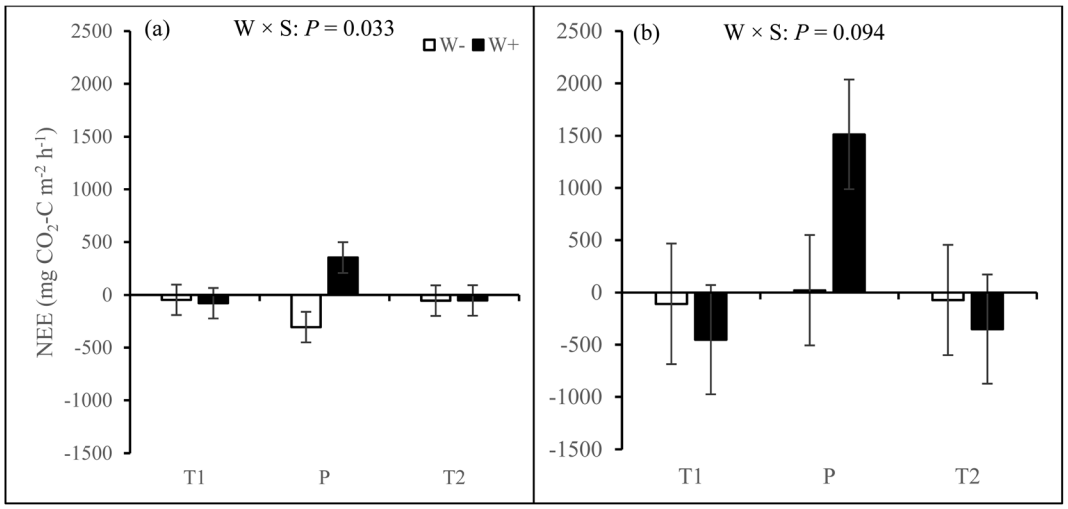

Fig. 2 Net ecosystem exchange (NEE) in mesocosms from T1, T2, and P sites under treatments with warming (W+, *i.e.* warming only and warming + increased cloudiness treatments) and without warming (W−, *i.e.* control and increased cloudiness only treatments) across five measurement campaigns in (a) the first and (b) second growing seasons. Bars represent season mean values (±SE, $n = 10$ per site per treatment). T = tundra, where T1 and T2 indicate the two locations within the tundra, and P = palsa mire. W × S = warming × site interaction. Statistically significant *P*-values < 0.05 and marginally significant *P*-values < 0.1 from LMM ANOVA are shown. See ESI_1 Tables S3 and S4† for detailed statistics.

measurement campaigns, and 51.8 ± 13.1 μg m^{-2} h^{-1} for the T1 site, 48.9 ± 10.8 μg m^{-2} h^{-1} for the T2 site, and 72.8 ± 10.3 μg m^{-2} h^{-1} for the P site. In the second growing season, control treatment total BVOC emissions averaged 58.2 ± 12.6 μg m^{-2} h^{-1} across all sites and measurement campaigns, and 67.3 ± 27.3 μg m^{-2} h^{-1} for the T1 site, 65.7 ± 23.8 μg m^{-2} h^{-1} for the T2 site, and 41.9 ± 12.7 μg m^{-2} h^{-1} for the P site.

During the first growing season, warming increased SQT (Fig. 3a) and OVOC (Fig. 3b) emissions across all sites. Warming effects on SQT emissions were most pronounced in the T1 and P sites (W × S × T interaction, see ESI_1 text, Table S3, and Fig. S9†). Warming also increased oMT emissions across all sites and the effect was significant in most measurement campaigns (W × T interaction, see ESI_1 text, Table S3, and Fig. S10†). Increased cloudiness mostly decreased oMT, other VOC, OVOC, and oSQT emissions (−PAR × S × T interaction, see ESI_1 text, Table S3, Fig. S11 and S12†). Across all sites, warming and increased cloudiness, in combination with each other, decreased OVOC and MT but mostly increased HC emissions in several measurement campaigns (W × −PAR × T interaction, see ESI_1 text, Table S3, and Fig. S13†).

Across all measurement campaigns during the second growing season, warming increased SQT emissions in all sites and the effects were most pronounced in the T1 and P sites (W

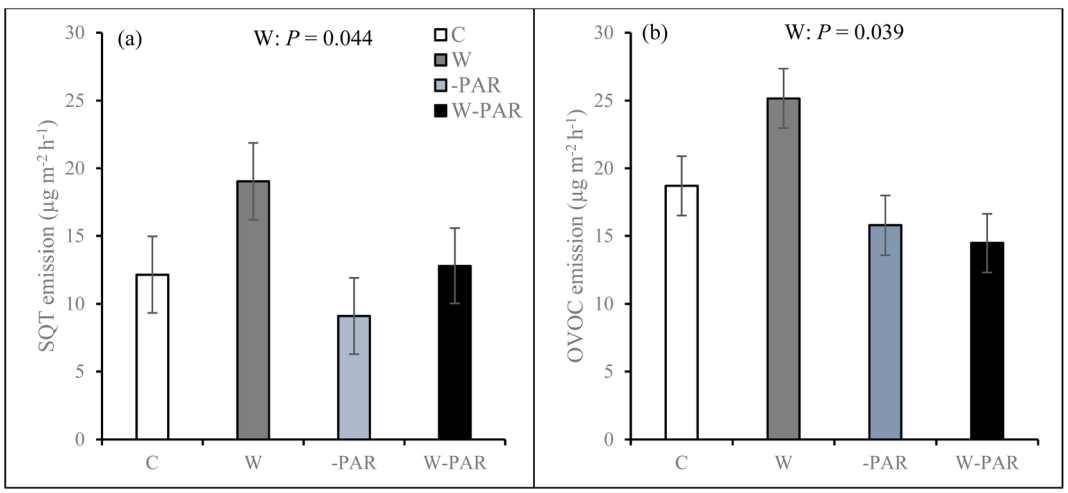

Fig. 3 (a) SQT and (b) OVOC emissions from mesocosms across all sites in control (C), warming (W), increased cloudiness (−PAR), and warming + increased cloudiness (W−PAR) treatments during the first growing season. Bars represent season mean values (±SE, $n = 15$ per treatment). W = warming treatments (W+, *i.e.* warming only and warming + increased cloudiness). Statistically significant *P*-values < 0.05 from LMM ANOVA are shown.

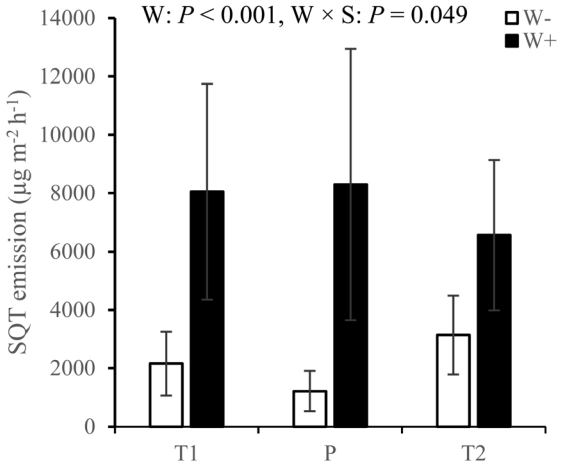

Fig. 4 SQT emissions from T1, T2 and P sites under treatments with warming (W+, *i.e.* warming only and warming + increased cloudiness treatments) and without warming (W−, *i.e.* control and increased cloudiness only treatments) during the second growing season. Bars represent season mean values (±SE, $n = 10$ per site per treatment). T = tundra, where T1 and T2 indicate the two locations within the tundra, and P = palsa mire. W = warming treatments (W+, *i.e.* warming only and warming + increased cloudiness), W × S = warming × site interaction. Statistically significant *P*-values < 0.05 from LMM ANOVA are shown. See ESI_1 Table S4† for detailed statistics.

× S, Fig. 4, see ESI_1 Table S4†). Warming increased MT emissions (Fig. 5a), significantly in the T1 and P sites and was dependent on measurement campaign (W × S × T interaction, see ESI_1 text, Table S4, and Fig. S14†). Warming also increased oMT and other VOC emissions across all sites, dependent on measurement campaign (W × T interaction, see ESI_1 text, Table S4, and Fig. S15†). Across all sites and measurement campaigns, HC emissions increased by 122.5% under increased cloudiness (Fig. 5b). Across all sites, increased cloudiness decreased the emissions of MT and other VOC, dependent on measurement campaign (−PAR × T interaction, see ESI_1 text, Table S4, and Fig. S16†). Increased cloudiness decreased isoprene emissions in the P site during several measurement campaigns (−PAR × S × T interaction, see ESI_1 text, Table S4, and Fig. S17†). Warming and increased cloudiness, in combination with each other, increased OVOC emissions but this was dependent on measurement campaign (W × −PAR × T interaction, see ESI_1 text, Table S4, and Fig. S18†).

3.6 Covariance between gas fluxes and vegetation and soil properties

According to the PLS regression on the first growing season data, ER was positively related to soil carbon and organic matter and negatively related to soil pH and bulk density, but the model was not significant (Fig. 6a, $P = 0.19$, CV-ANOVA). PLS regression also showed that GEP was positively related to soil bulk density, pH, and total organic carbon and negatively related to soil carbon and organic matter, but the model was not significant (Fig. 6b, $P = 0.21$, CV-ANOVA). Soil nitrate was positively related to N_2O emission (Fig. 6c). The only BVOC group which could be explained by the vegetation and soil properties was MT as the emission was positively related to evergreen shrubs and lichens cover, and soil water holding capacity and organic layer depth but negatively related to soil nitrogen (Fig. 6d).

The PLS regression on the second growing season data showed that ER was positively related to litter cover and soil carbon and negatively related to moss cover, and soil pH and bulk density (Fig. 7a). PLS regression also showed that GEP was positively related to moss cover, soil pH and total organic carbon and negatively related to the cover of litter and bare soil (Fig. 7b). The emission of N_2O was positively related to litter cover and soil ammonium and negatively related to the cover of lichens, deciduous shrubs, and mosses (Fig. 7c). Isoprene, OVOC, and oSQT were the BVOC groups that could be explained

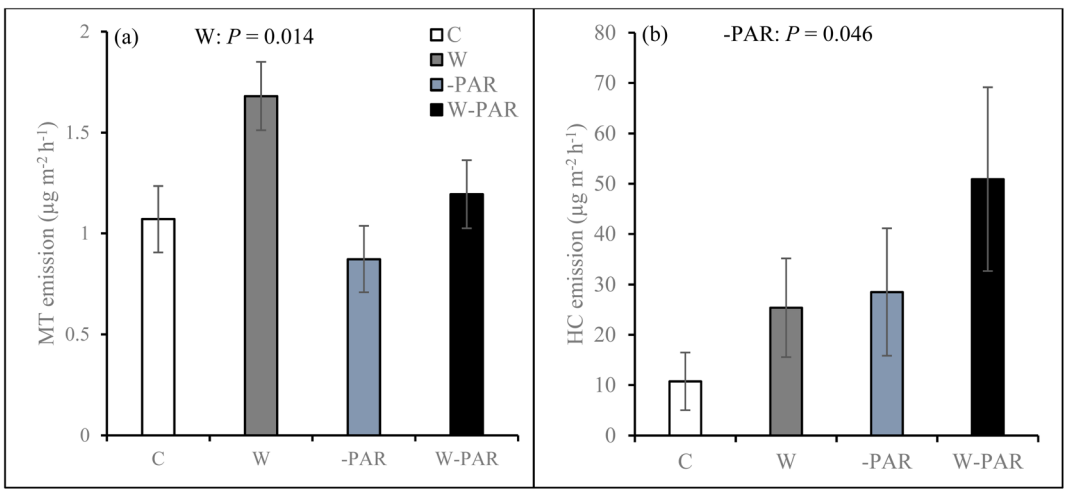

Fig. 5 (a) MT and (b) HC emissions from mesocosms across all sites in control (C), warming (W), increased cloudiness (−PAR), and warming + increased cloudiness (W−PAR) treatments during the second growing season. Bars represent season mean values (±SE, $n = 15$ per treatment). W = warming treatments (W+, *i.e.* warming only and warming + increased cloudiness), −PAR = increased cloudiness treatments (−PAR+, *i.e.* increased cloudiness only and warming + increased cloudiness). Statistically significant *P*-values < 0.05 from LMM ANOVA are shown.

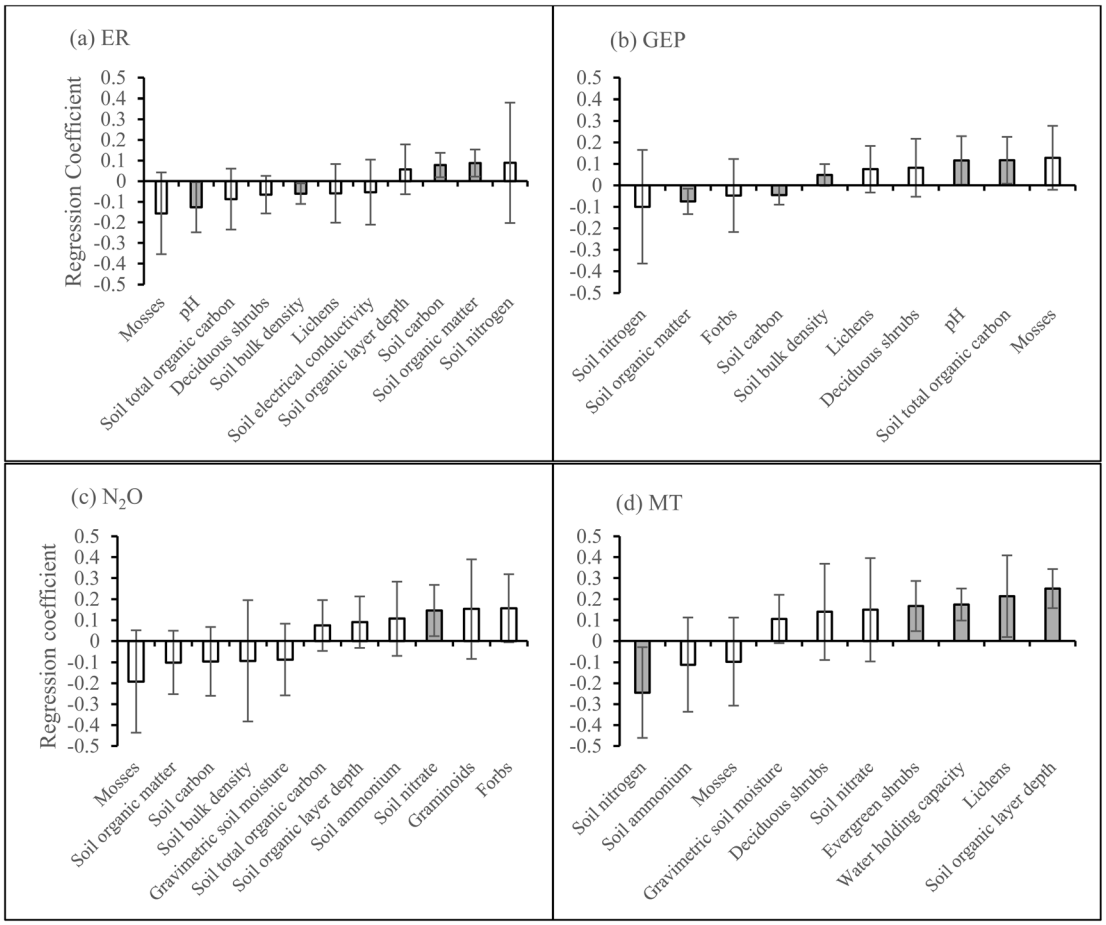

Fig. 6 Regression coefficients from PLS regression models on (a) ER, (b) GEP, (c) N_2O, and (d) MT during the first growing season. Error bars show ± 2 standard deviations of the regression coefficients. Significant variables are marked with grey bars. The shown models for N_2O and MTs are significant (CV-ANOVA) at $P < 0.05$.

by the vegetation or soil properties. Isoprene emission was positively related to the cover of bare soil and soil organic matter and negatively related to moss cover and gravimetric soil moisture (Fig. 7d). The emission of OVOC was positively related to the cover of graminoids and forbs (Fig. 7e) and oSQT emission with soil nitrate (Fig. 7f). No significant relationships were found between CH_4 flux and vegetation or soil properties during any of the growing seasons (ESI_1 Fig. S19†).

4. Discussion

We investigated the influence of the predicted warming and increased cloudiness conditions on the fluxes of GHGs and reactive trace gases in two tundra and one palsa mire ecosystems in climate simulation chambers. Our experiment ran over two growing seasons and allowed us to also assess whether and how prevailing vegetation and soil physiochemical properties affected the fluxes. The tundra and palsa sites were generally net sinks of CH_4 during both growing seasons. The tundra sites were also net sinks of CO_2 while the palsa site was generally a net source of CO_2. Warming increased CH_4 uptake and CO_2 emission (*i.e.* more positive NEE rates) in the P site and turned one of the tundra sites (T1) from a sink to a source of CH_4. Warming generally increased BVOC emissions while increased cloudiness decreased the emissions. The combined treatment of warming and increased cloudiness mostly decreased CH_4 uptake and BVOC emissions. The fluxes of N_2O were mainly driven by soil physiochemical properties and plant species composition. The emissions of NO and HONO were below detection limits.

4.1 Methane fluxes

The uptake rates of CH_4 in mesocosms from the tundra and palsa sites were comparable to, or lower than, fluxes measured from laboratory and *in situ* studies, including dry arctic heath,[52] dry arctic upland ecosystems,[7,53] dry arctic lowland tundra,[54] dry and moist arctic tundra,[11] dry bare and vegetated peat palsa surfaces,[55] and temperate forests.[9] The warming treatment increased CH_4 uptake and sink strength and the effects were mostly observed in the P site during both growing seasons. Higher temperatures due to warming may have accelerated the activity of CH_4 oxidizing bacteria, thereby enhancing CH_4 uptake.[5,56] In the second growing season, warming turned one of the tundra sites (T1) from a sink to a source of CH_4 indicating that methanogen activity dominated in this site under warming. It is important to mention here that mesocosms from the

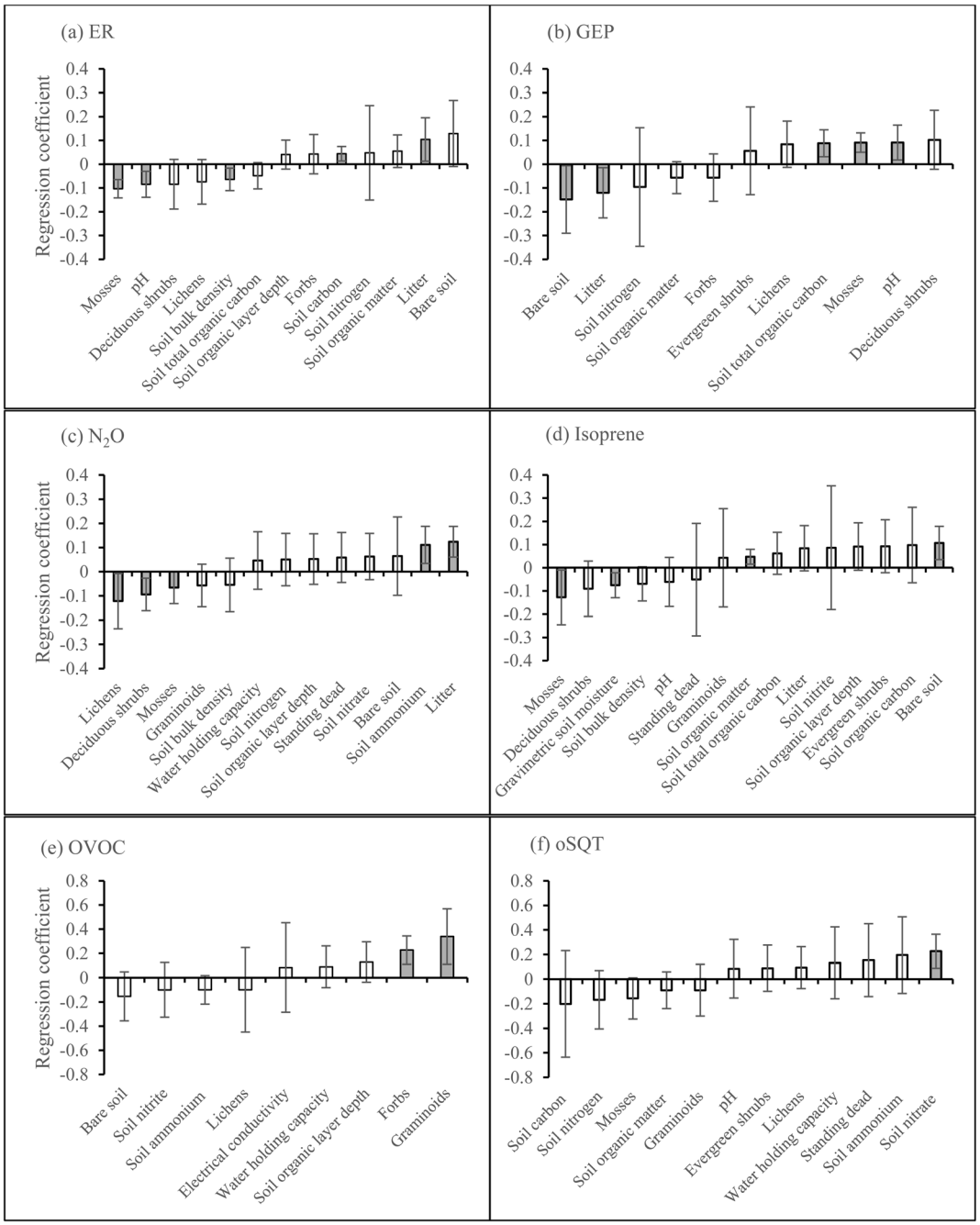

Fig. 7 Regression coefficients from PLS regression models on (a) ER, (b) GEP, (c) N_2O, (d) isoprene, (e) OVOC, and (f) oSQT during the second growing season. Error bars show ± 2 standard deviations of the regression coefficients. Significant variables are marked with grey bars. The shown models are significant (CV-ANOVA) at $P < 0.05$.

tundra sites (T1 and T2) were mostly made up of organic rather than mineral soil. This may have limited methanotroph activity in mesocosms from the tundra sites considering the critical role of mineral soils in CH_4 oxidation.[57] We found no main effects of increased cloudiness on CH_4 fluxes. However, increased cloudiness modified the responses to warming as CH_4 uptake decreased in the combined treatment. Reduced light availability simulating increased cloud cover may have offset soil warming and methanotroph activity, thereby reducing CH_4 uptake as was observed in the combined treatment during the first growing season. During the second growing season, the reduced light availability may have also offset warming effects almost to the point of balancing out CH_4 production and consumption across all sites as net CH_4 fluxes were near zero in the combined treatments. Soil moisture and permeability are important factors controlling CH_4 fluxes due to their impact on oxygen availability and gas diffusion through the soil.[7,9] However, in this study, the mesocosms were watered to maintain their initial weight and the soil moisture was not altered significantly. We also did not find any significant relationships between CH_4

fluxes and the soil gravimetric water content and bulk density. Additionally, soil pH, nutrient availability, and plant species composition contribute to regulating CH_4 fluxes in the soil–atmosphere interface.[5,7,9–12] We did not find any significant relationships between CH_4 fluxes and soil pH, soil nutrient, or plant species composition across all sites when data were aggregated across all sites and measurement campaigns for both growing seasons.

4.2 Carbon dioxide fluxes

The rates of CO_2 fluxes were within the range of fluxes measured from *in situ* studies carried out in subarctic ecosystems.[58–60] NEE was generally negative indicating net CO_2 uptake by all sites except that warming turned the P site from a sink to a source of CO_2 (positive NEE fluxes) in the first growing season and increased the source strength of the P site in the second growing season. While other studies have reported temperature to be an important driver of ER due to the control on microbial processes, decomposition, and bacterial growth,[3,39,58] the warming treatment in this study did not significantly affect ER rates. Despite light being an important factor controlling photosynthetic CO_2 uptake,[8,13] reduced light availability due to the increased cloudiness treatments had no significant effects on CO_2 fluxes. We also found no significant effects of combined warming and increased cloudiness treatments on CO_2 fluxes. The positive relationship of ER with litter and soil carbon and organic matter and negative relationship with moss cover and soil pH and bulk density during both growing seasons suggests vegetation and soil properties provided overriding controls of ER and GEP. For example, litter input coupled with available soil carbon and organic matter may have significant control on substrate availability, microbial activity, and soil respiration.[61] Increased litter input and bare soil cover and higher availability of soil carbon and organic matter in the P site characterized by peat soil may have enhanced ER rates compared to GEP rendering the P site a source of CO_2 as opposed to the tundra sites which were made up of podsol soil with higher soil bulk density and ground layer mostly covered with mosses. In addition, warming may affect ER rates indirectly through changes in vegetation cover or composition and quality and quantity of litter input,[62] ultimately influencing net CO_2 balance (NEE).

4.3 Fluxes of nitrous oxide, nitric oxide, and nitrous acid

The flux rates of N_2O were in the range of fluxes measured from *in situ* and laboratory studies, including moist and dry arctic lowland tundra,[54] and upland tundra and vegetated peat surfaces.[59,63–65] Recently, low NO and HONO emissions ($\leq$0.2 $\mu g\ N\ m^{-2}\ h^{-1}$ for both gases) were observed from vegetated surfaces of intact peat cores collected from subarctic permafrost peatlands at the Seida site in Russia and the Kilpisjärvi and Kevo sites in northern Finland.[66] In our study, the mesocosms showed low (below detection limit) NO and HONO fluxes. The availability of mineral nitrogen, mostly regulated by plant nitrogen uptake, is the major driver of N_2O, NO, and HONO emissions from soils, and the two main microbial processes generating N_2O, NO, and HONO in soils are nitrification and denitrification.[18,20,67] Previous studies have reported significant emissions of N_2O, NO, and HONO mostly from bare soils.[19,20,59,63–65] As opposed to bare soils, amounts of inorganic nitrogen are low in the vegetated soils limiting production of N_2O,[22,59,63–65] NO, and HONO.[66] The low N_2O, NO, and HONO fluxes as well as the absence of significant treatment effects in this study could therefore be explained by increased competition for mineral nitrogen by plants limiting available nitrogen for microbial N_2O, NO, and HONO production processes, such as nitrification and denitrification. On an ecosystem scale, plants have been shown to be involved in N_2O emissions from plant–soil systems.[68] However, the mechanisms by which plants alter N_2O emissions remains somewhat unclear as to whether N_2O is produced by the plants themselves,[68] or whether they serve as a conduit for the transport of N_2O produced in the soil to the atmosphere.[69] Whatever pathway of N_2O emissions by plants is involved, the negative relationship between N_2O emission and the cover of especially deciduous shrubs suggests vascular plants in the plant–soil system in this study had no positive control or effect on N_2O emissions. In addition, the negative relationship with moss and lichens could be as a result of these growth forms contributing very little to N_2O flux *via* evapotranspiration since they lack roots to take up N_2O found in soil water.[70] We found that N_2O emission was positively related to soil NO_3^- during the first growing season, and to litter and soil NH_4^+ during the second growing season. This suggests that the availability of mineral nitrogen coupled with increased litter input, which is expected to enhance mineral nitrogen availability through increased decomposition and mineralization, may promote N_2O emissions from subarctic soils.

4.4 Fluxes of biogenic volatile organic compounds

The total BVOC emission rates were lower than those measured *in situ* from vegetated palsa surfaces in a permafrost-affected peatland,[71] but were comparable to, or higher than, fluxes measured in other *in situ* studies, including a boreal forest floor,[72] vegetated boreal bog,[73] and subarctic *E. hermaphroditum*-dominated forest floor.[74] Increased emissions of BVOCs (*i.e.* SQTs and oMTs in both growing seasons, OVOCs in the first growing season, and MTs and other VOCs in the second growing season) in response to warming shows the temperature dependency of BVOC emissions from subarctic plants and ecosystems.[44,75,76] Decreased BVOC emissions (*i.e.* oMT, other VOC, OVOC and oSQT during the first growing season and MT, other VOC, and isoprene during the second growing season) in response to increased cloudiness also shows the light dependency of BVOC emissions from subarctic plants, soil, and ecosystems.[77] As BVOCs are regulated by temperature and light availability, their emissions may decrease, *e.g.* OVOC and MT during the first growing season, or increase, *e.g.* OVOC during the second growing season, in response to combined warming and increased cloudiness. The temperature and light dependency of BVOCs is linked to enzymatic regulation and photosynthetic activity.[47,78] *De novo* synthesized BVOCs, like isoprene and some monoterpenes, are usually directly linked to

photosynthetic activity.[79–81] The strong temperature dependency of the emission of BVOCs which are stored in specific storage compartments, like ducts or glandular trichomes, is a direct result of faster enzymatic reactions and compound volatilization from stored pools.[47,78] BVOCs may originate from soil microorganisms,[24,77,82–84] which can alter their activity pattern in response to increased temperatures or reduced light.

Although alterations in BVOC emissions may result from direct effect of temperature or reduced light availability,[77,85] the emissions may also be controlled by soil properties and plant species composition[82,84,86] which may change in response to increased temperature, reduced light, or nutrient availability. We found a negative relationship between MT emissions and soil nitrogen availability in the first growing season. Soil nitrogen availability may affect emissions of BVOCs (including MTs) by altering the pattern of carbon allocation between growth and the synthesis of carbon-based secondary metabolites such as BVOCs,[87,88] or by altering community of microbial decomposers involved in production of BVOCs at different stages of litter decomposition.[86] The positive relationship of isoprene emission with soil organic matter and negative relationship with gravimetric water content may be due to the influence of these soil properties on isoprene emitting plant species such as the graminoids *Carex vaginata* and *Deschampsia flexuosa* which were present especially in mesocosms from the tundra sites (T1 and T2).[49] Isoprene is also thought to be produced as a metabolite by soil microorganisms,[89] hence soil organic matter and gravimetric water content may influence microbial metabolism and production or consumption of isoprene.[89,90] Warming and/or increased cloudiness may alter the pattern of resource allocation between above- and belowground biomass, thereby modifying BVOC emission responses. For example, reduced light availability may favor allocation of resources to aboveground plant parts such as stems and leaves at the expense of roots, hence decreased soil emissions,[77] while emissions from aboveground plant parts may increase coupled with enhanced aboveground biomass due to warming.[82] Increased biomass of one of the dominant evergreen shrubs *E. hermaphroditum*, a MT emitter,[91] in response to warming,[49] may have contributed to the observed increased MT emissions under warming supported by the positive relationship between MT emissions and the cover of evergreen shrubs. In the second growing season, the combined treatment of warming and increased cloudiness significantly increased the cover of graminoids and forbs especially in the T1 site which was characterized with high abundance of these species.[49] The higher cover of graminoids and forbs could partly explain the increased OVOC emissions in the combined treatment during the second growing season, strengthened by the positive relationship between OVOC emissions and the cover of graminoids and forbs, as opposed to the first growing season where the emissions decreased in response to the combined treatment. The negative relationship between isoprene emissions and the cover of mosses is contrary to studies that have reported mosses as significant sources of isoprene,[92,93] but may indicate the potential of mosses, and denser vegetation cover, as sinks of isoprenoids,[94–96] since we observed a positive relationship between isoprene emissions and the cover of bare soil.

5. Implications, limitations, and future directions

Our results indicate that future warming and increased cloudiness conditions in the subarctic will alter GHG and reactive trace gas fluxes and the effects will be very pronounced in subarctic palsa mires. Enhanced CH_4 uptake under warming could be attributed to direct effects of the temperature increase on biotic process related to methanotrophs activity. Hence, subarctic ecosystems may play a significant role in mitigating warming effects by CH_4. However, CH_4 uptake was found to decrease under combined warming and increased cloudiness. Thus, if the climate warms coupled with increased cloud cover, subarctic ecosystems may in the long-term shift from sinks towards sources of CH_4 thereby exacerbating global warming. Warming enhanced the CO_2 source strength of the palsa site suggesting this ecosystem type may exacerbate global warming under future temperature increase. Fluxes of CO_2 were linked to the availability of soil carbon and organic matter, litter input, soil pH and bulk density, and the cover of mosses indicating controls of these soil properties and vegetation cover on the fluxes. Warming-induced BVOC emissions may enhance cloud formation through atmospheric aerosol formation, initiating a negative feedback mechanism between biosphere, aerosol, and climate since BVOC emissions are highly regulated by sunlight availability. In addition, enhanced climate warming associated with increased atmospheric lifetime of CH_4 due to increased BVOC emissions, which compared to CH_4 can be more readily oxidized by OH radicals, may be a minor issue. This is because increased BVOC emissions was accompanied by enhanced CH_4 uptake under warming. Fluxes of N_2O were not affected by the climate treatments while HONO and NO fluxes were below detection limit probably due to low availability of inorganic nitrogen. Predicting how the fluxes of GHG and reactive trace gases will change with climate change depends on the complex interactions between abiotic and biotic environmental changes over time, which could have important implications for subarctic climate feedbacks.

Our study involved climate chambers which allowed the simulation of combined effects of warming and increased cloudiness under highly controlled environmental conditions over two growing seasons. Quantifying trace gas responses to climate change using chamber experiments like in our study is challenging and accompanied by unavoidable uncertainties. Firstly, simulating cloud–aerosol–climate interactions and cloud radiative forcing in chamber experiments like in our study is challenging. Secondly, though we watered the mesocosms throughout the experimental duration to maintain their initial weight and soil moisture level, the soil gravimetric water content might have been slightly altered but with no direct effects on the gas fluxes. Thirdly, due to technical constraints, the fluxes of CH_4, N_2O, NO, and HONO were measured at room temperature that could influence to some extent underlying

mechanisms controlling the fluxes and might have led to an under or overestimation of the fluxes, the effect of which was the same across all treatments since mesocosms from all treatments were measured in the same manner. Finally, the analyses of soil physiochemical properties involved destructive analyses that could only be performed at the end of the experiment in the second growing season. However, the soil properties are unlikely to have been affected by the treatments during the two-years exposure period which is a relatively shorter time compared to the time taken for the formation of these soils at the field site. The next step in unravelling the effects of climate change on trace gas exchange in the high latitudes should be geared towards discriminating for the individual and combined effects of warming and increased cloudiness over a longer time span in field conditions. Future field studies could be extensive enough to allow destructive, simultaneous sampling of soil physiochemical properties and plant characteristics, along with trace gas flux measurements. Potential future work including projections of cloud formation through more sophisticated modelling techniques that include changes in land-surface physical characteristics, such as albedo which controls land–atmosphere interactions, are also needed to strengthen future predictions of climate change effects on trace gas exchange in the high latitudes.

Data availability

The data supporting the findings of this study have been included as part of the ESI.†

Author contributions

Flobert A. Ndah: conceptualization, formal analysis, funding acquisition, investigation, methodology, visualization, writing – original draft, writing – review and editing; Marja Maljanen: conceptualization, funding acquisition, methodology, project administration, resources, supervision, writing – review and editing; Riikka Rinnan: conceptualization, methodology, writing – review and editing; Hem Raj Bhattarai: formal analysis; investigation; methodology; writing – review and editing; Cleo L. Davie-Martin: formal analysis, methodology; Santtu Mikkonen: formal analysis; methodology; writing – review and editing; Anders Michelsen: conceptualization, methodology, writing – review and editing; Minna Kivimäenpää: conceptualization, formal analysis, funding acquisition, investigation, methodology, project administration, resources, supervision, writing – review and editing.

Conflicts of interest

Authors declare no conflicts of interest.

Appendices

Appendix A

Treatments performed in the climate chambers and their abbreviations

Abbreviation	Treatment
C	Control [ambient temperature and photosynthetically active radiation (PAR, thin-cloud conditions)]
W	Warming treatment [4 °C above ambient temperature and ambient PAR (thin-cloud conditions)]
−PAR	Increased cloudiness treatment [ambient temperature and 50% below ambient PAR (thick-cloud conditions)]
W−PAR	Warming and increased cloudiness combined [4 °C above ambient temperature and 50% below ambient PAR (thick-cloud conditions)]

Summary of all the main and interaction effects and one example simple main effects (SME) comparison in each category of main and interaction effects (statistical terms used in the text, tables, and figures of the main article and supplement) and their corresponding explanations or interpretations

Main/ interaction effect	SME comparison	Interpretation
W	—	W main effect irrespective of −PAR, S or time
−PAR	—	−PAR main effect irrespective of W, S or time
S	—	S main effect irrespective of W, −PAR or time
T	—	Time main effect irrespective of W, −PAR or S
W × S	W+ *vs.* W− in T1 site	Effect of W in T1 site irrespective of −PAR or time
W × T	W+ *vs.* W− in early July	Effect of W in early July of the growing season irrespective of −PAR or S
−PAR × T	−PAR+ *vs.* −PAR− in mid-June	Effect of −PAR in mid-June of the growing season irrespective of W or S
W × S × T	W+ *vs.* W− in T1 site and early July	Effect of W in T1 site in early July of the growing season irrespective of −PAR
−PAR × S × T	−PAR+ *vs.* −PAR- in T2 site and mid-June	Effect of −PAR in T2 site and mid-June of the growing season irrespective of W
W × −PAR × S	W+ *vs.* W− in −PAR− and P site	Effect of W in without −PAR treatment in P site irrespective of time
	−PAR+ *vs.* −PAR− in W+ and T1 site	Effect of −PAR in W treatment in T1 site irrespective of time
W × −PAR × T	W+ *vs.* W− in −PAR+ and mid-June	Effect of W in −PAR treatment in mid-June of the growing season irrespective of S
	−PAR+ *vs.* −PAR− in W+ and mid-June	Effect of −PAR in W treatment in mid-June of the growing season irrespective of S
W × −PAR × S × T	W+ *vs.* W− in −PAR−, T2 site and early July	Effect of W in without −PAR treatment in T2 site and early July of the growing season
	−PAR+ *vs.* −PAR− in W+, P site and mid-June	Effect of −PAR in W treatment in P site and mid-June of the growing season

Appendix B

Supplementary data.†

Acknowledgements

This research was funded by the Finnish Cultural Foundation and the Academy of Finland (Decision No. 348571, 352968). R. R. acknowledges the support by the Danish National Research Foundation for Center for Volatile Interactions (VOLT, DNRF168). We thank Timo Oksanen (Department of Environmental and Biological Sciences, University of Eastern Finland) for technical assistance, and Jaana Rissanen and Hanna Kenttä for their assistance in gas flux sampling.

References

1 S. E. Hobbie, K. J. Nadelhoffer and P. A. Högberg, A synthesis: The role of nutrients as constraints on carbon balances in boreal and arctic regions, *Plant Soil*, 2002, **242**, 163–170, DOI: 10.1023/A:1019670731128.

2 M. C. Mack, E. A. G. Schuur, M. S. Bret-Harte, G. R. Shaver and F. S. Chapin III, Ecosystem carbon storage in arctic tundra reduced by long-term nutrient fertilization, *Nature*, 2004, **432**, 440–443, DOI: 10.1038/nature02887.

3 E. A. Davidson and I. A. Janssens, Temperature sensitivity of soil carbon decomposition and feedbacks to climate change, *Nature*, 2006, **440**, 165–173, DOI: 10.1038/nature04514.

4 B. A. Ball, R. A. Virginia, J. E. Barrett, A. N. Parsons and D. H. Wall, Interactions between physical and biotic factors influence CO_2 flux in Antarctic dry valley soils, *Soil Biol. Biochem.*, 2009, **41**, 1510–1517, DOI: 10.1016/j.soilbio.2009.04.011.

5 K. R. Tate, Soil methane oxidation and land-use change—From process to mitigation, *Soil Biol. Biochem.*, 2015, **80**, 260–272, DOI: 10.1016/j.soilbio.2014.10.010.

6 S. C. Whalen, Biogeochemistry of methane exchange between natural wetlands and the atmosphere, *Environ. Eng. Sci.*, 2005, **22**, 73–94, DOI: 10.1089/ees.2005.22.73.

7 C. A. Emmerton, V. L. S. Louis, I. Lehnherr, E. R. Humphreys, E. Rydz and H. R. Kosolofski, The net exchange of methane with high Arctic landscapes during the summer growing season, *Biogeosciences*, 2014, **11**, 3095–3106, DOI: 10.5194/bgd-11-1673-2014.

8 S. Trumbore, Carbon respired by terrestrial ecosystems – recent progress and challenges, *Global Change Biol.*, 2006, **12**, 141–153, DOI: 10.1111/j.1365-2486.2006.01067.x.

9 K. A. Smith, K. E. Dobbie, B. C. Ball, L. R. Bakken, B. K. Sitaula, S. Hansen, *et al*, Oxidation of atmospheric methane in Northern European soils, comparison with other ecosystems, and uncertainties in the global terrestrial sink, *Global Change Biol.*, 2000, **6**, 791–803, DOI: 10.1046/j.1365-2486.2000.00356.x.

10 W. Chen, B. Wolf, X. Zheng, Z. Yao, K. Butterbach-Bahl, N. Brüggemann, *et al*, Annual methane uptake by temperate semiarid steppes as regulated by stocking rates, aboveground plant biomass and topsoil air permeability, *Global Change Biol.*, 2011, **17**, 2803–2816, DOI: 10.1111/j.1365-2486.2011.02444.x.

11 C. J. Jørgensen, K. M. Johansen, A. Westergaard-Nielsen and B. Elberling, Net regional methane sink in High Arctic soils of northeast Greenland, *Nat. Geosci.*, 2015, **8**, 20–23, DOI: 10.1038/NGEO2305.

12 L. Ström, J. M. Falk, K. Skov, M. Jackowicz-Korcynski, M. Mastepanov, T. R. Christensen, *et al*, Controls of spatial and temporal variability in CH_4 flux in a high arctic fen over three years, *Biogeochemistry*, 2015, **125**, 21–35, DOI: 10.1007/s10533-015-0109-0.

13 M. Magnani, I. Baneschi, M. Giamberini, B. Raco and A. Provenzale, Microscale drivers of summer CO_2 fluxes in the Svalbard High Arctic tundra, *Sci. Rep.*, 2022, **12**, 763, DOI: 10.1038/s41598-021-04728-0.

14 IPCC, Climate Change 2021: The Physical Science Basis, in *Contribution of Working Group I to the Sixth Assessment Report of the Intergovernmental Panel on Climate Change*, ed. V. Masson-Delmotte, P. Zhai, A. Pirani, S. L. Connors, C. Péan, S. Berger, N. Caud, Y. Chen, L. Goldfarb, M. I. Gomis, M. Huang, K. Leitzell, E. Lonnoy, J. B. R. Matthews, T. K. Maycock, T. Waterfield, O. Yelekçi, R. Yu and B. Zhou, Cambridge University Press, 2021, DOI: 10.1017/9781009157896.

15 R. Atkinson, Atmospheric chemistry of VOCs and NO*x*, *Atmos. Environ.*, 2000, **34**, 2063–2101, DOI: 10.1016/S1352-2310(99)00460-4.

16 Y. F. Elshorbany, J. Kleffmann, R. Kurtenbach, M. Rubio, E. Lissi, G. Villena, *et al*, Summertime photochemical ozone formation in Santiago, Chile, *Atmos. Environ.*, 2009, **43**, 6398–6407, DOI: 10.1016/j.atmosenv.2009.08.047.

17 K. Riedel and K. Lassey, Detergent of the atmosphere, *Water Atmos.*, 2008, **16**, 22–23.

18 M. Maljanen, P. Yli-Pirilä, J. Hytönen, J. Joutsensaari and P. J. Martikainen, Acidic northern soils as sources of atmospheric nitrous acid (HONO), *Soil Biol. Biochem.*, 2013, **67**, 94–97, DOI: 10.1016/j.soilbio.2013.08.013.

19 H. R. Bhattarai, P. Virkajärvi, P. Yli-Pirilä and M. Maljanen, Emissions of atmospherically important nitrous acid (HONO) gas from northern grassland soil increases in the presence of nitrite (NO_2^-), *Agric., Ecosyst. Environ.*, 2018, **256**, 194–199, DOI: 10.1016/j.agee.2018.01.017.

20 H. R. Bhattarai, W. Wanek, H. M. P. Siljanen, J. G. Ronkainen, M. Liimatainen, Y. Hu, *et al*, Denitrification is the major nitrous acid production pathway in boreal agricultural soils, *Commun. Earth Environ.*, 2021, **2**, 54, DOI: 10.1038/s43247-021-00125-7.

21 S. Medinets, U. Skiba, H. Rennenberg and K. Butterbach-Bahl, A review of soil NO transformation: associated processes and possible physiological significance on organisms, *Soil Biol. Biochem.*, 2015, **80**, 92–117, DOI: 10.1016/j.soilbio.2014.09.025.

22 J. Gil, M. E. Marushchak, T. Rütting, E. M. Baggs, T. Pérez, A. Novakovskiy, *et al*, Sources of nitrous oxide and the fate of mineral nitrogen in subarctic permafrost peat soils, *Biogeosciences*, 2022, **19**, 2683–2698, DOI: 10.5194/bg-19-2683-2022.

23 J. Peñuelas and J. Llusià, BVOCs: Plant defense against climate warming?, *Trends Plant Sci.*, 2003, **8**, 105–109, DOI: 10.1016/S1360-1385(03)00008-6.
24 J. Peñuelas, D. Asensio, D. Tholl, K. Wenke, M. Rosenkranz, B. Piechulla, *et al*, Biogenic volatile emissions from the soil, *Plant, Cell Environ.*, 2014, **37**, 1866–1891, DOI: 10.1111/pce.12340.
25 C. J. Frost, M. C. Mescher, J. E. Carlson and C. M. De Moraes, Plant Defense Priming against Herbivores: Getting Ready for a Different Battle, *Plant Physiol.*, 2008, **146**, 818–824, DOI: 10.1104/pp.107.113027.
26 M. Boy, P. Zhou, T. Kurtén, D. Chen, C. Xavier, P. Clusius, *et al*, Positive feedback mechanism between biogenic volatile organic compounds and the methane lifetime in future climates, *npj Clim. Atmos. Sci.*, 2022, **5**, 72, DOI: 10.1038/s41612-022-00292-0.
27 C. E. Scott, A. Rap, D. V. Spracklen, P. M. Forster, K. S. Carslaw, G. W. Mann, *et al*, The direct and indirect radiative effects of biogenic secondary organic aerosol, *Atmos. Chem. Phys.*, 2014, **14**, 447–470, DOI: 10.5194/acp-14-447-2014.
28 D. V. Spracklen, B. Bonn and K. S. Carslaw, Boreal forests, aerosols and the impacts on clouds and climate, *Philos. Trans. R. Soc., A*, 2008, **366**, 4613–4626, DOI: 10.1098/rsta.2008.0201.
29 ACIA, *Climate Impacts Assessment*, Cambridge University Press, New York, NY, USA, 2005.
30 J. Overland, E. Dunlea, J. E. Box, R. Corell, M. Forsius, V. Kattsov, *et al*, The urgency of arctic change, *Polar Sci.*, 2019, **21**, 6–13, DOI: 10.1016/j.polar.2018.11.008.
31 J. R. Norris, R. J. Allen, A. T. Evan, M. D. Zelinka, C. W. O'Dell and S. A. Klein, Evidence for climate change in the satellite cloud record, *Nature*, 2016, **536**, 72–75, DOI: 10.1038/nature18273.
32 E. A. G. Schuur, J. Bockheim, J. G. Canadell, E. Euskirchen, C. B. Field, S. V. Goryachkin, *et al*, Vulnerability of permafrost carbon to climate change: Implications for the global carbon cycle, *Bioscience*, 2008, **58**, 701–714, DOI: 10.1641/B580807.
33 A. D. McGuire, L. G. Anderson, T. R. Christensen, S. Dallimore, L. Guo, D. J. Hayes, *et al*, Sensitivity of the carbon cycle to Arctic climate change, *Ecol. Monogr.*, 2009, **79**, 523–555, DOI: 10.1890/08-2025.1.
34 M. Kramshøj, C. N. Albers, S. H. Svendsen, M. P. Björkman, F. Lindwall, R. G. Björk, *et al*, Volatile emissions from thawing permafrost soils are influenced by meltwater drainage conditions, *Global Change Biol.*, 2019, **25**, 1704–1716, DOI: 10.1111/gcb.14582.
35 E. Graglia, S. Jonasson, A. Michelsen, I. K. Schmidt, M. Havström and L. Gustavsson, Effects of environmental perturbations on abundance of subarctic plants after three, seven and ten years of treatments, *Ecography*, 2001, **24**, 5–12, DOI: 10.1034/j.1600-0587.2001.240102.x.
36 S. C. Elmendorf, G. H. R. Henry, R. D. Hollister, R. G. Björk, N. Boulanger-Lapointe, E. J. Cooper, *et al*, Plot-scale evidence of tundra vegetation change and links to recent summer warming, *Nat. Clim. Change*, 2012, **2**, 453–457, DOI: 10.1038/nclimate1465.
37 F. S. Chapin III, M. Sturm, M. C. Serreze, J. P. McFadden, J. R. Key, A. H. Lloyd, *et al*, Role of land-surface changes in arctic summer warming, *Science*, 2005, **310**, 657–660, DOI: 10.1126/science.1117368.
38 J. H. C. Cornelissen, P. M. van Bodegom, R. Aerts, T. V. Callaghan, R. S. P. Van Logtestijn, J. Alatalo, *et al*, Global negative vegetation feedback to climate warming responses of leaf litter decomposition rates in cold biomes, *Ecol. Lett.*, 2007, **10**, 619–627, DOI: 10.1111/j.1461-0248.2007.01051.x.
39 R. Rinnan, A. Michelsen, E. Bååth and S. Jonasson, Mineralization and carbon turnover in subarctic heath soil as affected by warming and additional litter, *Soil Biol. Biochem.*, 2007, **39**, 3014–3023, DOI: 10.1016/j.soilbio.2007.05.035.
40 R. Rinnan, A. Michelsen and S. Jonasson, Effects of litter addition and warming on soil carbon, nutrient pools, and microbial communities in a subarctic heath ecosystem, *Appl. Soil Ecol.*, 2008, **39**, 271–281, DOI: 10.1016/j.apsoil.2007.12.014.
41 Y. Zhang, N. Zhang, Y. Jingjing, Y. Zhao, F. Yang, Z. Jiang, *et al*, Simulated warming enhances the responses of microbial N transformations to reactive N input in a Tibetan alpine meadow, *Environ. Int.*, 2020, **141**, 105795, DOI: 10.1016/j.envint.2020.105795.
42 P. Tiiva, P. Faubert, A. Michelsen, T. Holopainen, J. K. Holopainen and R. Rinnan, Climatic warming increases isoprene emission from a subarctic heath, *New Phytol.*, 2008, **180**, 853–863, DOI: 10.1111/j.1469-8137.2008.02587.x.
43 P. Faubert, P. Tiiva, Å. Rinnan, A. Michelsen, J. K. Holopainen and R. Rinnan, Doubled volatile organic compound emissions from subarctic tundra under simulated climate warming, *New Phytol.*, 2010, **187**, 199–208, DOI: 10.1111/j.1469-8137.2010.03270.x.
44 R. Seco, T. Holst, C. L. Davie-Martin, T. Simin, A. Guenther, N. Pirk, *et al*, Strong isoprene emission response to temperature in tundra ecosystems, *Proc. Natl. Acad. Sci. U. S. A.*, 2022, **119**, e2118014119, DOI: 10.1073/pnas.2118014119.
45 G. Stanhill and S. Cohen, Global dimming: a review of the evidence for a widespread and significant reduction in global radiation with discussion of its probable causes and possible agricultural consequences, *Agric. For. Meteorol.*, 2001, **107**, 255–278, DOI: 10.1016/S0168-1923(00)00241-0.
46 M. Kejna, J. Uscka-Kowalkowska and P. Kejna, The influence of cloudiness and atmospheric circulation on radiation balance and its components, *Theor. Appl. Climatol.*, 2021, **144**, 823–838, DOI: 10.1007/s00704-021-03570-8.
47 J. Laothawornkitkul, J. E. Taylor, N. D. Paul and C. N. Hewitt, Biogenic volatile organic compounds in the Earth system, *New Phytol.*, 2009, **183**, 27–51, DOI: 10.1111/j.1469-8137.2009.02859.x.
48 R. K. Monson and D. Baldocchi, Fluxes of biogenic volatile compounds between plants and the atmosphere, in

Terrestrial Biosphere-Atmosphere Fluxes, Cambridge University Press, New York, NY, USA, 2014, pp. 395–414, DOI: 10.1017/CBO9781139629218.

49 F. A. Ndah, M. Maljanen, A. Kasurinen, R. Rinnan, A. Michelsen, T. Kotilainen, *et al*, Acclimation of subarctic vegetation to warming and increased cloudiness, *Plant-Environ. Interact.*, 2024, **5**, e10130, DOI: 10.1002/pei3.10130.

50 A. J. Underwood, Analysis of variance, in *Experiments in Ecology: Their Logical Design and Interpretation Using Analysis of Variance*, Cambridge University Press, Cambridge, 1996, pp. 140–197, DOI: 10.1017/CBO9780511806407.007.

51 L. Eriksson, J. Trygg and S. Wold, CV-ANOVA for significance testing of PLS and OPLS® models, *J. Chemom.*, 2008, **22**, 594–600, DOI: 10.1002/cem.1187.

52 L. D'Imperio, C. S. Nielsen, A. Westergaard-Nielsen, A. Michelsen and B. Elberling, Methane oxidation in contrasting dry soil types: Responses to warming with implication for landscape-integrated CH_4 budget, *Global Change Biol.*, 2017, **23**, 966–976, DOI: 10.1111/gcb.13400.

53 J. R. Christiansen, A. J. B. Romero, N. O. G. Jørgensen, M. A. Glaring, C. J. Jørgensen, L. K. Berg, *et al*, Methane fluxes and the functional groups of methanotrophs and methanogens in a young Arctic landscape on Disko Island, West Greenland, *Biogeochemistry*, 2014, **122**, 15–33, DOI: 10.1007/s10533-014-0026-7.

54 Q. Chen, R. Zhu, Q. Wang and H. Xu, Methane and nitrous oxide fluxes from four tundra ecotopes in Ny-Ålesund of the High Arctic, *J. Environ. Sci.*, 2014, **26**, 1403–1410, DOI: 10.1016/j.jes.2014.05.005.

55 C. Voigt, M. Marushchak, M. Mastepanov, R. E. Lamprecht, T. R. Christensen, M. Dorodnikov, *et al*, Ecosystem carbon response of an Arctic peatland to simulated permafrost thaw, *Global Change Biol.*, 2019, **25**, 1746–1764, DOI: 10.1111/gcb.14574.

56 Y. Zhou, F. Hagedorn, C. Zhou, X. Jiang, X. Wang and M.-H. Li, Experimental warming of a mountain tundra increases soil CO_2 effluxes and enhances CH_4 and N_2O uptake at Changbai Mountain, China, *Sci. Rep.*, 2016, **6**, 21108, DOI: 10.1038/srep21108.

57 A. Saari, J. Heiskanen and P. J. Martikainen, Effect of the organic horizon on methane oxidation and uptake in soil of a boreal Scots pine forest, *FEMS Microbiol. Ecol.*, 1998, **26**(3), 245–255, DOI: 10.1111/j.1574-6941.1998.tb00509.x.

58 E. P. Pedersen, B. Elberling and A. Michelsen, Seasonal variations in methane fluxes in response to summer warming and leaf litter addition in a subarctic heath ecosystem, *J. Geophys. Res.: Biogeosci.*, 2017, **122**, 2137–2153, DOI: 10.1002/2017JG003782.

59 C. Voigt, R. E. Lamprecht, M. E. Marushchak, S. E. Lind, A. Novakovskiy, M. Aurela, *et al*, Warming of subarctic tundra increases emissions of all three important greenhouse gases – carbon dioxide, methane, and nitrous oxide, *Global Change Biol.*, 2017, **23**, 3121–3138, DOI: 10.1111/gcb.13563.

60 O. A. Mikhaylov, S. V. Zagirova and M. N. Miglovets, Seasonal and inter-annual variability of carbon dioxide exchange at a boreal peatland in north-east European Russia, *Mires Peat*, 2019, **24**, 1–16, DOI: 10.19189/MaP.2017.OMB.293.

61 Y. Zhang, J. Zou, D. Meng, S. Dang, J. Zhou, B. Osborne, *et al*, Effect of soil microorganisms and labile C availability on soil respiration in response to litter inputs in forest ecosystems: A meta-analysis, *Ecol. Evol.*, 2020, **10**, 13602–13612, DOI: 10.1002/ece3.6965.

62 S. L. Maes, J. Dietrich, G. Midolo, S. Schwieger, M. Kummu, V. Vandvik, *et al*, Environmental drivers of increased ecosystem respiration in a warming tundra, *Nature*, 2024, **629**, 105–113, DOI: 10.1038/s41586-024-07274-7.

63 M. E. Repo, S. Susiluoto, S. E. Lind, S. Jokinen, V. Elsakov, C. Biasi, *et al*, Large N_2O emissions from cryoturbated peat soil in tundra, *Nat. Geosci.*, 2009, **2**, 189–192, DOI: 10.1038/ngeo434.

64 M. E. Marushchak, A. Pitkämäki, H. Koponen, C. Biasi, M. Seppälä and P. J. Martikainen, Hot spots for nitrous oxide emissions found in different types of permafrost peatlands, *Global Change Biol.*, 2011, **17**, 2601–2614, DOI: 10.1111/j.1365-2486.2011.02442.x.

65 C. Voigt, M. E. Marushchak, R. E. Lamprecht, M. Jackowicz-Korczynski, A. Lindgren, M. Mastepanov, *et al*, Increased nitrous oxide emissions from Arctic peatlands after permafrost thaw, *Proc. Natl. Acad. Sci. U. S. A.*, 2017, **114**, 6238–6243, DOI: 10.1073/pnas.1702902114.

66 H. R. Bhattarai, M. E. Marushchak, J. Ronkainen, R. E. Lamprecht, H. M. Siljanen, P. J. Martikainen, *et al*, Emissions of atmospherically reactive gases nitrous acid and nitric oxide from Arctic permafrost peatlands, *Environ. Res. Lett.*, 2022, **17**, 024034, DOI: 10.1088/1748-9326/ac4f8e.

67 K. Butterbach-Bahl, E. M. Baggs, M. Dannenmann, R. Kiese and S. Zechmeister-Boltenstern, Nitrous oxide emissions from soils: how well do we understand the processes and their controls?, *Philos. Trans. R. Soc. London, Ser. B*, 2013, **368**, 20130122, DOI: 10.1098/rstb.2013.0122.

68 C. Müller, Plants affect the *in situ* N_2O emissions of a temperate grassland ecosystem, *J. Plant Nutr. Soil Sci.*, 2003, **166**, 771–773, DOI: 10.1002/jpln.200321201.

69 M. Pihlatie, P. Ambus, J. Rinne, K. Pilegaard and T. Vesala, Plant-mediated nitrous oxide emissions from beech (*Fagus sylvatica*) leaves, *New Phytol.*, 2005, **168**, 93–98, DOI: 10.1111/j.1469-8137.2005.01542.x.

70 K. J. Stewart, M. E. Brummell, R. E. Farrell and S. D. Siciliano, N_2O flux from plant–soil systems in polar deserts switch between sources and sinks under different light conditions, *Soil Biol. Biochem.*, 2012, **48**, 69–77, DOI: 10.1016/j.soilbio.2012.01.016.

71 Y. Jiao, C. L. Davie-Martin, M. Kramshøj, C. T. Christiansen, H. Lee, I. H. J. Althuizen, *et al*, Volatile organic compound release across a permafrost-affected peatland, *Geoderma*, 2023, **430**, 116355, DOI: 10.1016/j.geoderma.2023.116355.

72 M. Wang, G. Schurgers, H. Hellèn, F. Lagergren and T. Holst, Biogenic volatile organic compound emission from a boreal forest floor, *Boreal Environ. Res.*, 2018, **23**, 249–265.

73 E. Männistö, H. Ylänne, M. Losoi, M. Keinänen, P. Yli-Pirilä, A. Korrensalo, *et al.*, Emissions of biogenic volatile organic compounds from adjacent boreal fen and bog as impacted

by vegetation composition, *Sci. Total Environ.*, 2023, **858**, 159809, DOI: 10.1016/j.scitotenv.2022.159809.

74 P. Faubert, P. Tiiva, A. Michelsen, Å. Rinnan, H. Ro-Poulsen and R. Rinnan, The shift in plant species composition in a subarctic mountain birch forest floor due to climate change would modify the biogenic volatile organic compound emission profile, *Plant Soil*, 2012, **352**, 199–215, DOI: 10.1007/s11104-011-0989-2.

75 T. Simin, J. Tang, T. Holst and R. Rinnan, Volatile organic compound emission in tundra shrubs – dependence on species characteristics and the near-surface environment, *Environ. Exp. Bot.*, 2021, **184**, 104387, DOI: 10.1016/j.envexpbot.2021.104387.

76 T. Li, N. Baggesen, R. Seco and R. Rinnan, Seasonal and diel patterns of BVOC fluxes in a subarctic tundra, *Atmos. Environ.*, 2023, **292**, 119430, DOI: 10.1016/j.atmosenv.2022.119430.

77 M. Kramshøj, I. Vedel-Petersen, M. Schollert, Å. Rinnan, J. Nymand, H. Ro-Poulsen, *et al*, Large increases in Arctic biogenic volatile emissions are a direct effect of warming, *Nat. Geosci.*, 2016, **9**, 349–352, DOI: 10.1038/ngeo2692.

78 F. Loreto and J. P. Schnitzler, Abiotic stresses and induced BVOCs, *Trends Plant Sci.*, 2010, **15**, 154–166, DOI: 10.1016/j.tplants.2009.12.006.

79 F. Loreto and T. D. Sharkey, A gas-exchange study of photosynthesis and isoprene emission in *Quercus rubra* L, *Planta*, 1990, **182**, 523–531, DOI: 10.1007/BF02341027.

80 C. F. Delwiche and T. D. Sharkey, Rapid appearance of ^{13}C in biogenic isoprene when $^{13}CO_2$ is fed to intact leaves, *Plant, Cell Environ.*, 1993, **16**, 587–591, DOI: 10.1111/j.1365-3040.1993.tb00907.x.

81 F. Loreto, P. Ciccioli, A. Cecinato, E. Brancaleoni, M. Frattoni and D. Tricoli, Influence of Environmental Factors and Air Composition on the Emission of [alpha]-Pinene from Quercus ilex Leaves, *Plant Physiol.*, 1996, **110**(1), 267–275, DOI: 10.1104/pp.110.1.267.

82 H. Valolahti, M. Kivimäenpää, P. Faubert, A. Michelsen and R. Rinnan, Climate change-induced vegetation change as a driver of increased subarctic biogenic volatile organic compound emissions, *Global Change Biol.*, 2015, **21**, 3478–3488, DOI: 10.1111/gcb.12953.

83 E. Bourtsoukidis, T. Behrendt, A. M. Yañez-Serrano, H. Hellén, E. Diamantopoulos, E. catão, *et al*, Strong sesquiterpene emissions from Amazonian soils, *Nat. Commun.*, 2018, **9**, 2226, DOI: 10.1038/s41467-018-04658-y.

84 S. H. Svendsen, A. Priemé, J. Voriskova, M. Kramshøj, M. Schostag, C. S. Jacobsen, *et al*, Emissions of biogenic volatile organic compounds from arctic shrub litter are coupled with changes in the bacterial community composition, *Soil Biol. Biochem.*, 2018, **120**, 80–90, DOI: 10.1016/j.soilbio.2018.02.001.

85 A. Ghirardo, F. Lindstein, K. Koch, F. Buegger, M. Schloter, A. Albert, *et al*, Origin of volatile organic compound emissions from subarctic tundra under global warming, *Global Change Biol.*, 2020, **26**, 1908–1925, DOI: 10.1111/gcb.14935.

86 X. Huang, L. Zheng, P. Guo and Z. Yi, Nitrogen addition inhibits total monoterpene emissions in subtropical forest floor of South China, *Soil Ecol. Lett.*, 2021, **3**, 63–72, DOI: 10.1007/s42832-020-0056-0.

87 J. P. Bryant, F. S. Chapin and D. R. Klein, Carbon/nutrient balance of boreal plants in relation to vertebrate herbivory, *Oikos*, 1983, **40**, 357–368, DOI: 10.2307/3544308.

88 M. Lerdau, M. Litvak and R. Monson, Plant chemical defense: monoterpenes and the growth-differentiation balance hypothesis, *Trends Ecol. Evol.*, 1994, **9**, 58–61, DOI: 10.1016/0169-5347(94)90269-0.

89 S. Mancuso, C. Taiti, N. Bazihizina, C. Costa, P. Menesatti, L. Giagnoni, *et al*, Soil volatile analysis by proton transfer reaction-time of flight mass spectrometry (PTR-TOF-MS), *Appl. Soil Ecol.*, 2015, **86**, 182–191, DOI: 10.1016/j.apsoil.2014.10.018.

90 J. Tang, G. Schurgers and R. Rinnan, Process understanding of soil BVOC fluxes in natural ecosystems: A review, *Rev. Geophys.*, 2019, **57**, 966–986, DOI: 10.1029/2018RG000634.

91 I. Vedel-Petersen, M. Schollert, J. Nymand and R. Rinnan, Volatile organic compound emission profiles of four common arctic plants, *Atmos. Environ.*, 2015, **120**, 117–126, DOI: 10.1016/j.atmosenv.2015.08.082.

92 D. T. Hanson, S. Swanson, L. E. Graham and T. D. Sharkey, Evolutionary significance of isoprene emission from mosses, *Am. J. Bot.*, 1999, **86**, 634–639, DOI: 10.2307/2656571.

93 I. Ryde, C. L. Davie-Martin, T. Li, M. P. Naursgaard and R. Rinnan, Volatile organic compound emissions from subarctic mosses and lichens, *Atmos. Environ.*, 2022, **290**, 119357, DOI: 10.1016/j.atmosenv.2022.119357.

94 H. Aaltonen, J. Aalto, P. Kolari, M. Pihlatie, J. Pumpanen, M. Kulmala, *et al*, Continuous VOC flux measurements on boreal forest floor, *Plant Soil*, 2013, **369**, 241–256, DOI: 10.1007/s11104-012-1553-4.

95 M. Mäki, J. Heinonsalo, H. Hellén and J. Bäck, Contribution of understorey vegetation and soil processes to boreal forest isoprenoid exchange, *Biogeosciences*, 2017, **14**, 1055–1073, DOI: 10.5194/bg-14-1055-2017.

96 M. Kivimäenpää, J.-M. Markkanen, R. P. Ghimire, T. Holopainen, M. Vuorinen and J. K. Holopainen, Scots pine provenance affects the emission rate and chemical composition of volatile organic compounds of forest floor, *Can. J. For. Res.*, 2018, **48**, 1373–1381, DOI: 10.1139/cjfr-2018-0049.